J Therm Anal Calorim (2015) 120:1799–1810
DOI 10.1007/s10973-015-4511-6

Synthesis and crystallization behavior of novel poly(butylene succinate) copolyesters containing phosphorus pendent groups

Cheng Zhou · Zhiyong Wei · Yang Yu · Yang Li

Received: 12 October 2014 / Accepted: 29 January 2015 / Published online: 3 March 2015

Abstract Novel biodegradable poly(butylene succinate) (PBS) copolyesters containing phosphors flame-retardant groups were synthesized by melt-polycondensation from succinic acid and 9,10-dihydro-10-[2,3-di(hydroxycarbonyl)propyl]-10-phosphaphenanthrene-10-oxide (DDP) with 1,4-butanediol. In order to analyze the effects of the third monomer (DDP) on the relative properties of PBS, the composition, crystal structure, crystallization behavior, multiple melting behavior, and spherulitic morphology of the copolyesters were investigated by ^{1}H-NMR, WAXD, DSC, and POM, respectively. WAXD data revealed that the crystal structure of PBS was not affected by DDP. The overall crystallization kinetic showed that the crystallization of PBS was retarded with the introduction of DDP, especially when the DDP content exceeds 7.5 mol%, which may result from the stereo-hindrance of DDP unit. Furthermore, crystallization temperature (T_c), crystallization enthalpy (ΔH_c), melting temperature (T_m), and crystallinity (X_c) of PBS copolyesters also decreased apparently with the increase in DDP contents. Also, the equilibrium melting temperature (T_m^o) obtained from Hoffman-Weeks analysis decreased, indicating that the regularity of PBS chain segments was reduced probably due to the diluent effect of the specific chain structure of DDP. All spherulites showed the ring-banded extinction patterns, which implied that phosphorus-containing (DDP) segment did not change the growth mechanism of PBS crystals.

C. Zhou · Z. Wei · Y. Yu · Y. Li (✉)
State Key Laboratory of Fine Chemicals, Department of Polymer Science and Materials, School of Chemical Engineering, Dalian University of Technology, Dalian 116024, China
e-mail: liyang@dlut.edu.cn

Keywords Poly(butylene succinate) · Crystallization · Melting behavior · Phosphorus containing

Introduction

In recent decades, the energy and environmental problems have stimulated increasing interest in biodegradable polymers as green materials due to its excellent biodegradability, melt processability, and thermal and chemical resistance. Aliphatic polyesters, one of the most promising classes of environmentally friendly polymers in agricultural, sanitary fields, and packaging applications, are gaining continuous attention. Poly(butylene succinate) (PBS), a kind of typical biodegradable thermoplastic with similar properties to PE, is receiving more and more attention [1–4]. However, its flammability has restricted further applications of PBS.

In order to reduce combustibility and avoid the fire threat, flame retardants are necessary for the most polymeric materials. The most common flame retardants are inorganic or organic flame retardants; magnesium hydroxide [$Mg(OH)_2$], silicon dioxide (SiO_2), halogen/nitrogen/phosphorus-containing flame retardants are typical examples of flame retardants [5, 6]. The method of blending an additive-type flame retardant has the advantages of convenience and low manufacturing cost. However, the non-reactive flame retardant may migrate from the materials, which result in a bad flame retardation [7–10]. So, incorporating a reactive flame retardant into the polymer chains has been a current issue. Compared with the halogen-containing flame retardants, no toxic gas released for that containing phosphorus groups. Two series of phosphorus-containing copolyesters were synthesized by Chang et al. [11]. Results showed that the thermal stability

of copolyesters decreased when the phosphorus linkage was incorporated into the main chain, while for that having the phosphorus linkage as a pendant group, the thermal stability was improved. Both types of copolyesters have a trend showing lower melting point as the phosphors unit content increased, but the crystallization and melting behaviors of these copolyesters were not analyzed. Additionally, the phosphoryl trichloride was incorporated into the PLA backbone via the chain-extending reactions by Wang et al. [12]. They found that the M_n of PPLA did not have an obvious increase, but PPLA exhibits excellent flame retardancy with the increasing content of phosphorus. Even more exciting, PPLA can be used as a flame retardant for PLA due to its similar structures and only 5 mass% of PPLA can impart PLA a good flame-retardant property. Sablong et al. [13] synthesized a series of PBT copolyesters via SSP. The incorporation of DOPO-containing diol (DOPO–HQ–GE) significantly improved flame-retardant properties as well.

Recently, a novel phosphorus-containing compound 9,10-dihydro-10-[2,3-di(hydroxylcarbonyl) propyl]-10-phosphaphenanthrene-10-oxide, which usually abbreviated as DDP, is gaining increasing popularity due to its particular reactive properties and good flame retardancy [8, 14–19]. Undoubtedly, phosphorus-containing flame retardants have excellent flame retardancy. When burning, the phosphorus flame retardants can be decomposed into phosphoric acid, and then protective layer is formed to resist the higher temperatures and shields the underlying polymer from attack by oxygen and radiant heat. A reactive flame-retardant unsaturated polyester resin with enhanced thermal stability and excellent flame retardance, which meets the UL 94 V0 rating and achieved an LOI value of 29 when 1.62 % phosphorus was incorporated, was synthesized from a phosphorus-containing diacid(DDP) by Zhang et al. [7]. Chang et al. [8] synthesized a series of novel flame-retardant PET-co-PEDDP copolyesters. The introduction of DDP has improved the thermal stability and flame retardancy, and data show that LOI values of copolyesters are all greater than 33. However, few attentions were paid to the effects of DDP on the crystallization and melting behaviors of the resultant copolyesters. Generally, the phys-chemical properties, the biodegradability, the crystallization, and melting behaviors of the copolyesters are depended on the polymer composition and crystallinity. Hence, investigations of the crystallization and melting behaviors are crucial for establishing the structure–property relationships. Chen et al. [18, 19] introduced the DDP into the poly(trimethylene terephthalate) (PTT) copolyesters and studied the effect of DDP on the crystallization behaviors of PTT. Their results showed that the copolymer with more DDP content possesses a lower crystallization capacity, lower melting point, and a higher glass transition temperature.

To the best of our knowledge, there is no report on synthesis and properties of poly(butylene succinate) copolyesters containing DDP unit. In this paper, we firstly synthesized poly(butylene succinate) copolyesters containing DDP via melt-polycondensation. Then, we systemically investigated the effects of DDP on the crystallization kinetics, multiple behavior, crystal structure, and spherulitic morphology of PBS copolyesters.

Experimental

Materials

Succinic acid (SA, >99.5 %) was obtained from Guanfu Fine Chemical Research Institute, Tianjin, China. 1,4-Butanediol (BD, >97 %) was supplied by Sinopharm Chemical Reagent Co. Ltd. Stannous Octoate ($Sn(Oct)_2$, >96 %) was purchased from J&K chemical reagent. 9,10-dihydro-10-[2,3-di(hydroxycarbonyl) propyl]-10-phosphaphenanthrene-10-oxide (DDP) was purchased from Ousilei Chemicals Industry, Co. Ltd, Shouguang, China. All materials were used as received.

Sample preparation

The copolyesters were synthesized by a two-step polymerization (the synthesis route was depicted in Fig. 1). The molar ratio of BD/(SA + DDP) was 1.05/1, and appropriate amount of $Sn(Oct)_2$ was used as catalyst. During the first stage, the mixture was heated to 180 °C and reacted 3–4 h under nitrogen atmosphere to complete the esterification process. Then the pressure was reduced to 100 Pa; meanwhile, the temperature was raised to 230 °C for 2–3 h to remove the byproduct and the unreacted monomers. Finally, the product was dissolved in chloroform and precipitated with ethanol several times, then dried at 20 °C in vacuum for 24 h. The content of DDP ranged from 0 to 10 mol% (0, 2.5, 5, 7.5, 10 mol%) of the whole amount of di-acid, which were named as PBS0, PBS2.5, PBS5, PBS7.5, PBS10, respectively. Subsequently, the intrinsic viscosity of copolyesters was measured, and the viscosity-average molecular weights calculated by the Eq. (1) were listed in Table 1.

Intrinsic viscosity

The intrinsic viscosity of the polymers was measured by Ubbelohde viscometer at a concentration of 0.1 g dL^{-1} in chloroform at 30 °C. The viscosity-average molecular

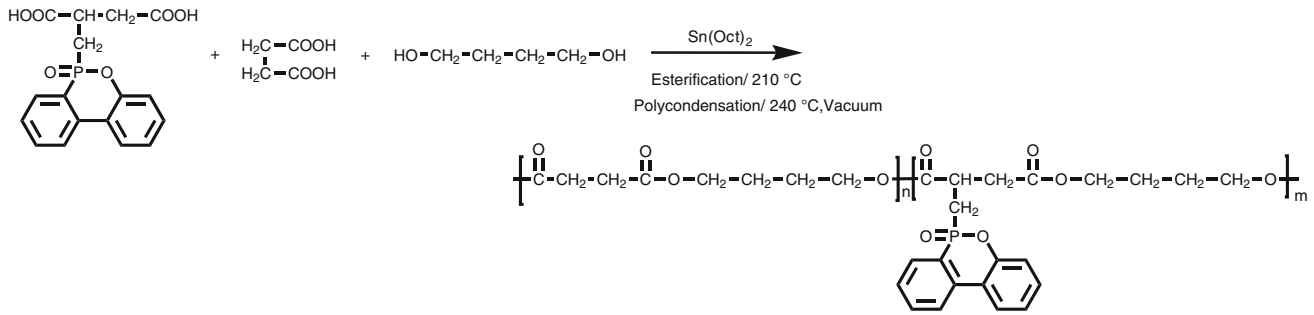

Fig. 1 Synthesis route of PBS copolyesters

Table 1 Composition and intrinsic viscosity of PBS copolyesters

Sample	In feed		Polymer composition[a]		$[\eta]$/dL g^{-1}	M_v/kDa[b]
	SA/mol%	DDP/mol%	SA/mol%	DDP/mol%		
PBS	100	0	100	0	0.58	14.2
PBS2.5	97.5	2.5	95.7	4.3	0.48	10.6
PBS5	95	5	93.0	7.0	0.40	8.0
PBS7.5	92.5	7.5	90.4	9.6	0.47	10.3
PBS10	90	10	89.0	11.0	0.36	6.8

[a] Calculated by ^{1}H-NMR

[b] Calculated by the Eq. (1) [20]

masses (M_v) of the products were calculated by using the Berkowitz equation [20]:

$$M_v = 3.29 \times 10^4 [\eta]^{1.54} \quad (1)$$

Proton nuclear magnetic resonance spectra (^{1}H-NMR)

All samples were recorded by a Bruker Avance 400 MHz spectrometer. Deuterated chloroform ($CDCl_3$) and tetramethylsilane (TMS) were used as a solvent and the calibration, respectively.

Wide-angle X-ray diffraction (WAXD)

All samples were performed on a Dmax-Ultima + X-ray diffractometer (Rigaku, Japan) with Ni-filtered Cu/K-α radiation ($\lambda = 0.15418$ nm). The operating target voltage was 40 kV, and the tube current was 100 mA. The scanning speed was 1.2° min^{-1} from 10° to 30°.

Differential scanning calorimetry (DSC)

Isothermal crystallization process was implemented in DSC1 (Mettler Toledo, Switzerland) differential scanning calorimeter. The instrument was calibrated using high-purity indium and zinc. Each sample (6–10 mg) was heated to 140 °C at the rate of 10 °C min^{-1}, keeping the temperature 5 min to remove the previous thermal history, then quenched to the indicated temperature to complete the crystallization process at the rate of −40 °C min^{-1}. Crystallization temperature (T_c), melting temperature (T_m), and crystallization enthalpy (ΔH_c) were recorded.

Temperature-modulated differential scanning calorimetry (TMDSC)

The samples were firstly isothermally crystallized at 80 °C temperatures for 30 min, followed by quenching to room temperature for TMDSC measurements, respectively. TMDSC measurements were performed with a TA instruments temperature-modulated DSC Q2000 (TA, USA) under nitrogen atmosphere at a heating rate of 3 °C min^{-1} with temperature modulation amplitude of 0.5 °C and modulation period of 60 s.

Polarized optical microscopy (POM)

The spherulite morphologies of PBS and its copolyesters were observed with a Leica 4500P polarized optical microscope (Germany) with a Linkam THMS600 hot stage. Thin films of samples were sandwiched between two thin glass slides, and then quenched to T_c after melted at 140 °C for 5 min, and maintained indicated time to observe the crystallization process.

Results and discussion

Copolymer composition and crystal structure

The chemical structures of PBS copolyesters characterized by ^{1}H-NMR are shown in Fig. 2. There are three characteristic peaks located at 4.12 (Proton b), 2.63 (Proton c), 1.70 (Proton a) ppm, which are consistent with the relative report [21]. The peak at 4.12 and 1.75 ppm are assigned to the –O–C$\underline{H}_2$– and the –O–CH$_2$–C$\underline{H}_2$– protons of BD unit, respectively, while the signal at 2.63 ppm represents the proton in –O–CO–C$\underline{H}_2$– of SA unit. From the Fig. 2b, we can see that several small peaks emerge from 7 to 8 ppm, which are ascribed to the –C$\underline{H}_2$– protons of benzene of DDP unit. So PBS copolyesters containing phosphorus groups are synthesized successfully in our laboratory. The molar percent of SA unit in PBS copolyesters could be calculated according to the equation as follow:

$$F_{\mathrm{DDP}} = 1 - \frac{I_{\mathrm{c}}}{I_{\mathrm{b}}} \tag{2}$$

where F_{DDP} is the molar fraction of DDP unit, I_{b} and I_{c} represent the integrals of the corresponding peaks, respectively. The obtained values are summarized in Table 1.

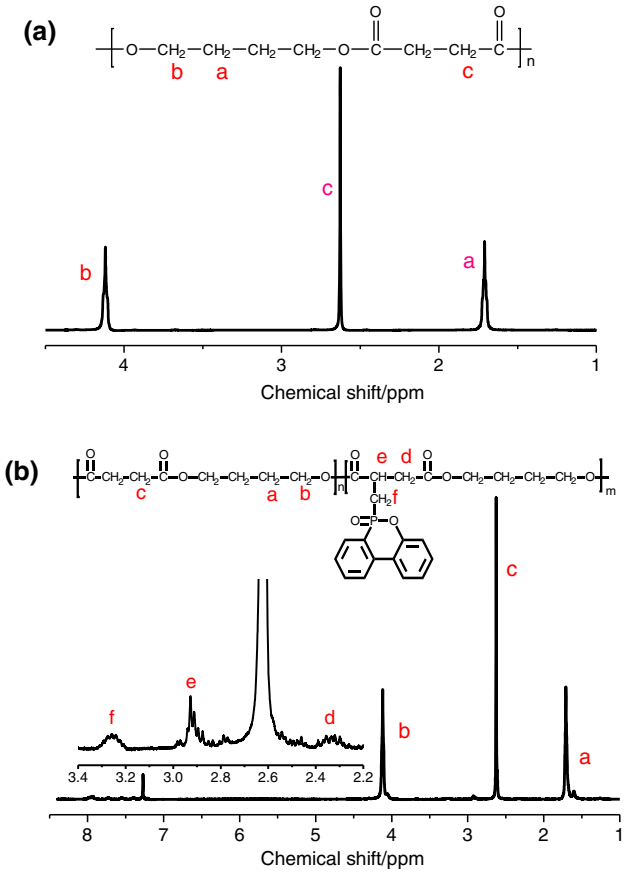

Fig. 2 ^{1}H-NMR spectra of **a** PBS and **b** PBS5

It is obviously found that the content of SA unit in copolyesters is lower than the feeding value, which resulted from the volatilization loss of succinic acid during polymerization process; the similar phenomenon has been found in the synthesis of poly(butylene succinate-co-lactic acid) copolyesters [22].

The crystal structures of PBS copolyesters are investigated with WAXD. Just as illustrated in Fig. 3, four peaks located at 19.3°, 21.7°, 22.4°, 28.7° are corresponding to the (020), (021), (110), and (111) planes of α-form PBS crystal, respectively [23]. All peaks for PBS copolyesters appear at the same location and conform that the crystal structure is almost not affected by the incorporation of the third component. However, the intensities of the main peaks decrease with the increasing content of DDP, suggesting that the crystallization of PBS segment is confined due to the large steric hindrance of DDP unit.

Thermal parameters of copolyesters

Thermal properties of copolyesters depend greatly on the polymer composition and crystallinity, so it is important to investigate the thermal ability of materials. All DSC procedures are conducted at a heating or cooling rate of 10 °C min^{-1} for PBS and its copolyesters. Figure 4 shows the DSC cooling (a) and subsequently heating (b) traces of copolyesters. For neat PBS, the crystallization temperature is 70.9 °C, and the intensity of the peak is sharper than other peaks for its copolyesters, indicating that the crystallization ability of neat PBS is depressed with the increases in DDP content. Additionally, with increasing the content of DDP from 2.5 to 10 mol%, the intensity of the crystallization peak decreases, and the values of crystallization temperature (T_{c}) shift from 65.9 to 40.8 °C. Furthermore, the values of melt crystallization enthalpy (ΔH_{c})

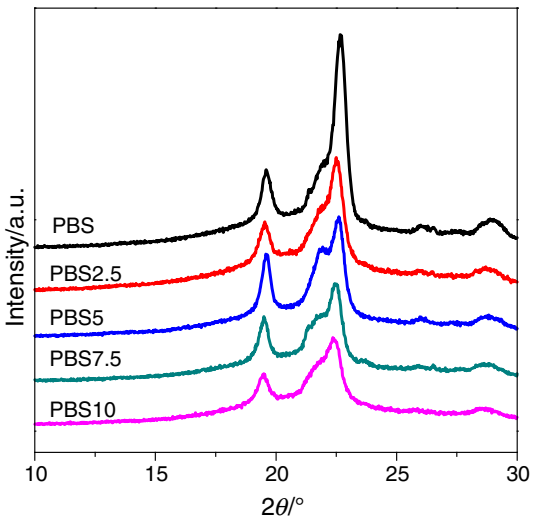

Fig. 3 WAXD patterns of neat PBS and its copolyesters

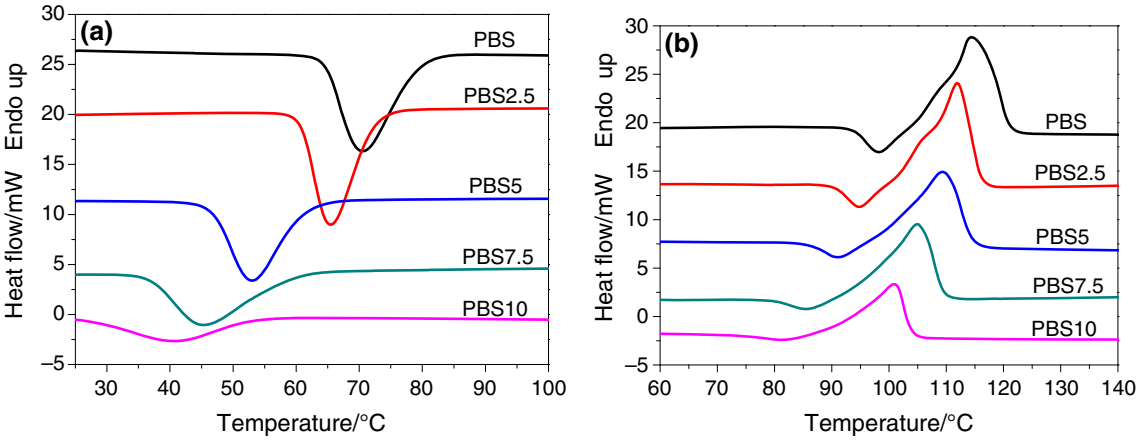

Fig. 4 DSC **a** cooling and **b** second heating scans by 10 °C min^{-1}

are also found to be dependent on the composition of DDP. For neat PBS, the value is 68.8 J g^{-1}, while ΔH_c for copolyesters decreases from 59.7 to 22.9 J g^{-1} compared with that of PBS. Crystallinity of neat PBS and its copolyesters was calculated by the equation:

$$X_c = \frac{\Delta H_c}{\Delta H_c^o} \times 100\,\% \tag{3}$$

where ΔH_c is the melt crystallization enthalpy measured by DSC and ΔH_c^o is the enthalpy for the complete crystallization. The value of ΔH_c^o is 200 J g^{-1} as reported by others [24].

From the subsequently heating traces in Fig. 4b, we can know that the values of T_m decrease with an increase in the content of DDP, and neat PBS has a final melting temperature (T_m) of 114.1 °C, while the values ranged from 111.5 to 100.7 °C for its copolyesters due to the increasing amount of imperfect crystals. Additionally, an exothermic peak (T_{exo}) prior to T_m is observed for all copolyesters, and T_{exo} shifts to lower temperature with the increase in DDP. The peak becomes less sharp and disappears finally when the content of DDP reaches 10 mol%. It is attributed to the recrystallization of the melting of the crystals with low stability [25], evidenced by TMDSC results later. All thermal parameters of copolyesters have been listed in Table 2. It is obvious that relative properties of PBS are affected by the incorporation of DDP, for example, both T_c and T_m are lower than that of neat PBS. Furthermore, the intrinsic viscosity decreases with the increasing content of DDP due to the hindering effect of the specific chain structure of DDP.

Table 2 Relative thermal parameters of PBS copolyesters

Sample	T_c/°C	X_c/%	ΔH_c/J g^{-1}	T_{exo}/°C	T_m/°C	T_m^o/°C
PBS	70.9	34.4	68.8	98.2	114.1	119.3
PBS2.5	65.9	29.8	59.7	95.0	111.5	115.6
PBS5	53.3	26.7	53.3	91.0	109.0	112.0
PBS7.5	45.7	26.3	52.5	85.7	104.8	108.2
PBS10	40.8	11.4	22.9	81.5	100.7	106.2

Isothermal crystallization kinetics

It is important to investigate the temperature on the crystallization rates and mechanism of PBS copolyesters in detail. The crystallization exotherms for PBS and PBS5 are shown in Fig. 5. Obviously, with the isothermal crystallization temperature increasing, the crystallization peak becomes broader, which means that the rate of the crystallization becomes slower. In addition, the intervals of isothermal crystallization for PBS and PBS5 are 84–90 and 70–76 °C, respectively; the obvious shift from higher temperature to lower temperature reveals that the addition of DDP hinders the crystallization process of PBS matrix due to the stereo-hindering effects.

Based on the assumption that the evolution of crystallinity is linearly proportional to the evolution of heat released during the crystallization, the relative degree of crystallinity, X_t, is determined as following:

$$X_t = \frac{X_t(t)}{X_t(\infty)} = \frac{\int_0^t (dH_c/dt)dt}{\int_0^\infty (dH_c/dt)dt} \tag{4}$$

where dH_c/dt is the rate of heat flow. Figure 6a shows the relative degree of crystallinity with time for isothermal crystallization at different temperatures of PBS5. All curves show the similar S-shape tendency. The time needed for completing the crystallization process with higher temperature increases, indicating that the crystallization is retarded with increasing crystallization temperature, which is consistent with the results that described in Fig. 5. Generally, the half time of crystallization at 50 % relative

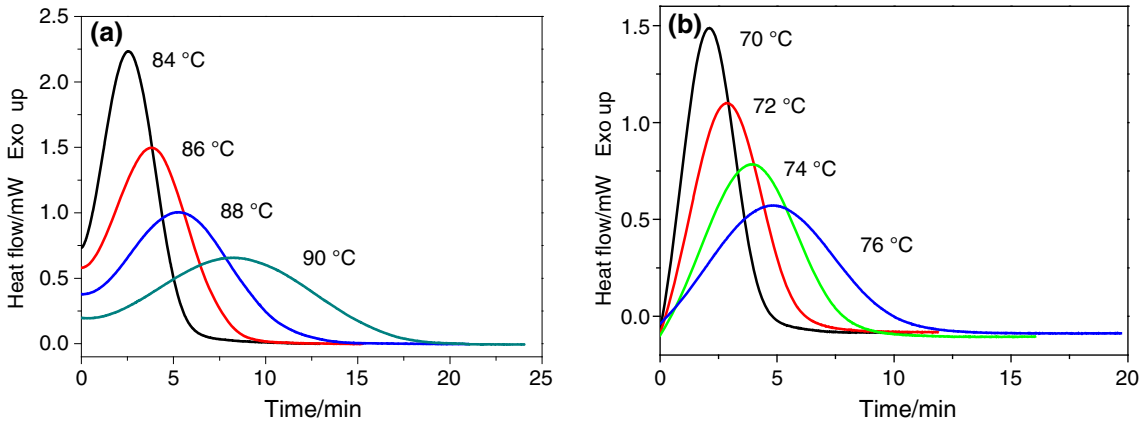

Fig. 5 DSC curves of isothermal crystallization at different temperatures: **a** PBS, **b** PBS5

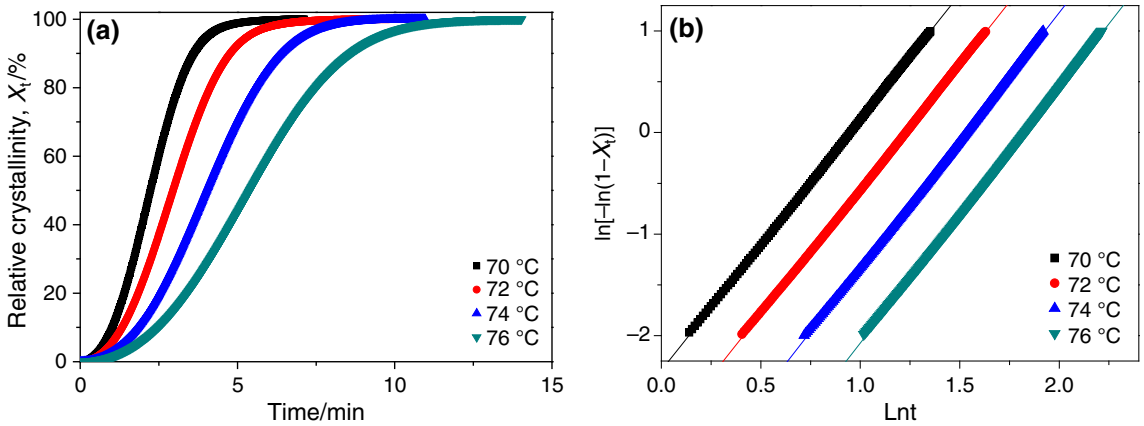

Fig. 6 **a** Relative degree of crystallinity with time and **b** Avrami plots of ln[−ln(1 − X_t)] versus ln$t$ of PBS5 for isothermal crystallization at different temperatures

crystallinity ($t_{1/2}$) is always used to evaluate the rate of the crystallization. The longer the $t_{1/2}$ is, the slower the crystallization processes. Relative isothermal parameters have been listed in Table 3. It is evident that at a given temperature (e.g., 86 °C), the values of $t_{1/2}$ are 3.29 and 6.80 min for PBS and PBS 2.5, respectively; more time was used to complete the crystallization process because of the hindering effects of DDP incorporated. The similar trend also can be found between PBS5 and PBS7.5 at 70 °C, PBS7.5 and PBS10 at 64 °C. Figure 7a, b illustrates the variations of $t_{1/2}$ and $1/t_{1/2}$ with T_c for PBS copolyesters, respectively. Just as depicted in Fig. 7a, for neat PBS and its copolyesters, values of $t_{1/2}$ increase with increasing temperature, suggesting that the isothermal crystallization process may be a nucleation-controlled process. In addition, the values of $t_{1/2}$ for neat PBS are smaller than that for its copolyesters at a given temperature, indicating that the crystallization process is retarded. From Fig. 7b, we can find the same trend that the values of $1/t_{1/2}$ decrease with the increases in crystallization temperature, which means the crystallization rates are reduced with the increasing content of DDP unit. The reduced overall crystallization rates may be attributed to the following two factors: Firstly, DDP content exerts a diluent influence for the crystallizable BS unit because of its larger steric hindrance, which will retard the crystallization process of PBS segments. Secondly, the equilibrium melting point temperature of PBS decreases with the increases in DDP content, indicating a decreasing driving force of the crystallization process, which would also result in a slower rate [19].

Avrami model is frequently used to describe the isothermal kinetics for many polymers [1, 3, 26, 27]. Just as the theory depicted, the relative crystallinity is a function of time, so the Avrami equation can be defined as follow:

$$X_t = 1 - \exp\left(-kt^n\right) \quad (5)$$

where n is the Avrami exponent depending on the mechanism of nucleation and the growth geometry of crystals, and k is a rate constant on crystallization, which is

Table 3 Results of the Avrami analysis for isothermal crystallization of PBS and its copolyesters

Sample	T_c/°C	K/min^{-n}	$t_{1/2}$/min	n	n (average)
PBS	84	0.118	2.35	2.11	2.09
	86	0.060	3.29	2.08	
	88	0.026	4.84	2.10	
	90	0.011	7.51	2.08	
PBS2.5	80	0.101	2.22	2.45	2.56
	82	0.037	3.18	2.55	
	84	0.013	4.65	2.63	
	86	0.005	6.80	2.60	
PBS5	70	0.096	2.23	2.47	2.49
	72	0.049	2.95	2.46	
	74	0.021	4.02	2.52	
	76	0.010	5.38	2.52	
PBS7.5	64	0.079	2.57	2.34	2.34
	66	0.040	3.42	2.36	
	68	0.019	4.62	2.36	
	70	0.011	6.08	2.30	
PBS10	58	0.077	2.73	2.18	2.15
	60	0.053	3.30	2.17	
	62	0.034	4.10	2.16	
	64	0.025	5.07	2.08	

related to nucleation. Generally speaking, the Avrami equation has always been modified as following:

$$\ln[-\ln(1 - X_t)] = \ln k + n \ln t \quad (6)$$

The Avrami plots of $\ln[-\ln(1 - X_t)]$ versus $\ln t$ for isothermal crystallization of PBS5 at different temperatures are illustrated in Fig. 6b. We can see that all cures show a good linear relationship within that range, which means the Avrami equation could explain the isothermal crystallization process of PBS and its copolyesters well. The values of n and k obtained from the fitting curves are summarized in Table 3. For each sample, with the increases in crystallization temperature, the values of k decrease obviously. T_c varies for all copolyesters; however, n values change little, which range from 2.08 to 2.63, indicating the three-dimensional growth of the crystal. So the incorporation of the third monomer does not change the nucleation mechanism and the geometry of crystal growth.

Multiple melting behavior and equilibrium melting point

Subsequent melting behaviors of PBS copolyesters are further studied by DSC. Figure 8 shows the melting curves recorded at 10 °C min^{-1} of PBS and PBS5 after isothermal crystallization at the indicated temperatures. As shown in Fig. 8, four characteristic peaks appear, which are labeled as T_a, T_{m1}, T_{exo}, T_{m2}, respectively. Here, we take PBS5 as an example to analyze the multi-melting behaviors of PBS copolyesters. T_a increases from 74.9 to 80.6 °C, and the fitting curves of T_a versus T_c are almost parallel to the line of $T_m = T_c$, which is the typical characteristic of an annealing peak [3]. T_{m1} and T_{exo} increase with the increased isothermal crystallization temperature, while the values of T_{m2} are almost constant.

From the result of XRD, we can know that the structure of crystal is not changed, so the multiple melting peaks are probably ascribed to the "melting-recrystallization-remelting" model [24, 28–30]. Melting of the crystals formed during the isothermal crystallization process leads to the appearance of the peak T_{m1}, and T_{m2} attributes to the melting of crystals formed through the recrystallization with the increasing of temperature. It is easier to see that the values of T_{m2} are independent on the temperature; the reason for the phenomenon may be explained as follows: the perfection and stability of crystals reach the top degree after the recrystallization

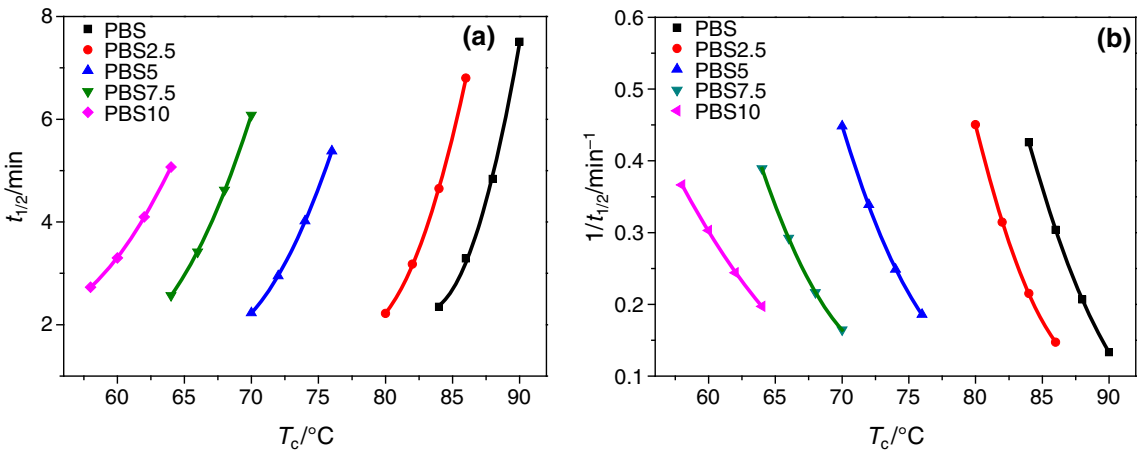

Fig. 7 Values of **a** $t_{1/2}$ and **b** $1/t_{1/2}$ of PBS copolyesters at various crystallization temperatures

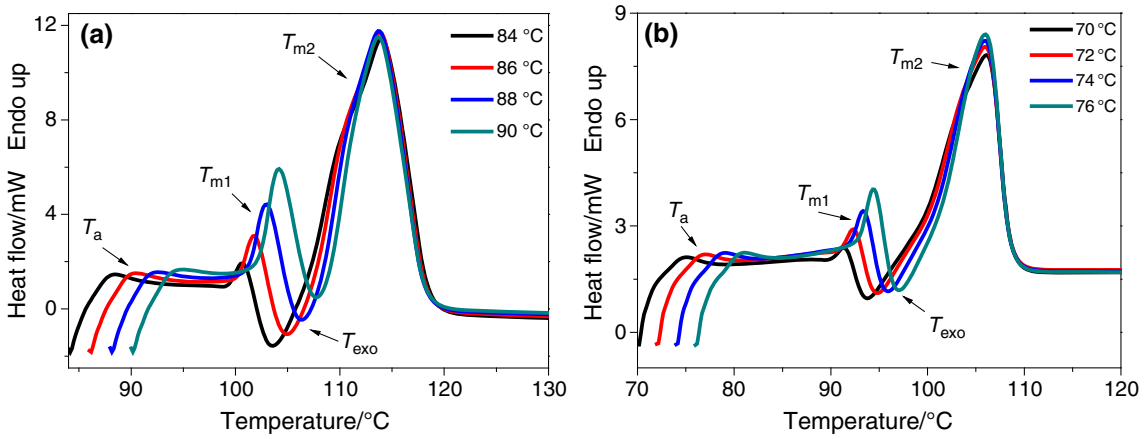

Fig. 8 DSC heating scans recorded at 10 °C min^{-1} of **a** PBS, **b** PBS5 after isothermal crystallization at indicated temperatures

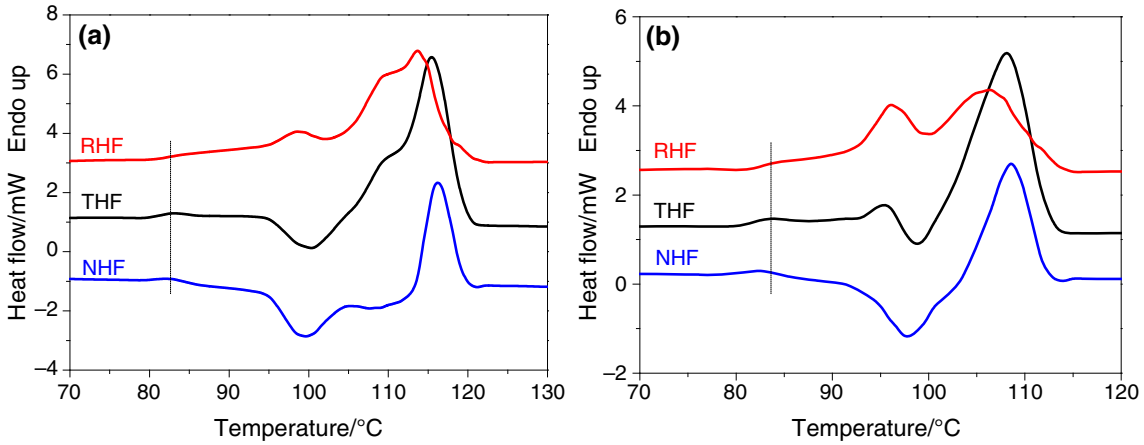

Fig. 9 Total heat flow (THF), reversible heat flow (RHF), and nonreversible heat flow (NHF) *curves* in TMDSC traces for **a** PBS and **b** PBS5 crystallized at 80 °C for 30 min. Heating rate was 3 °C min^{-1} with a modulation amplitude of 0.5 °C in a period of 60 s

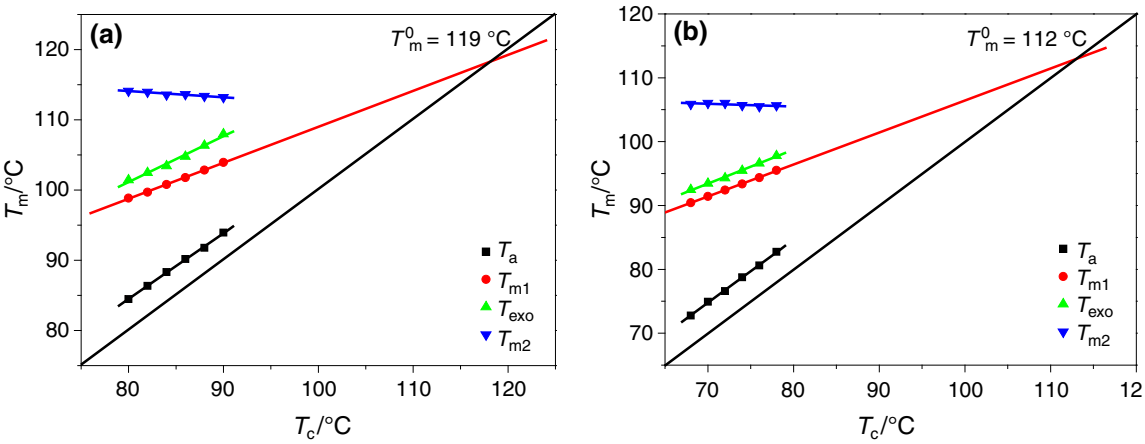

Fig. 10 Dependence of melting point on crystallization temperature: **a** PBS and **b** PBS5

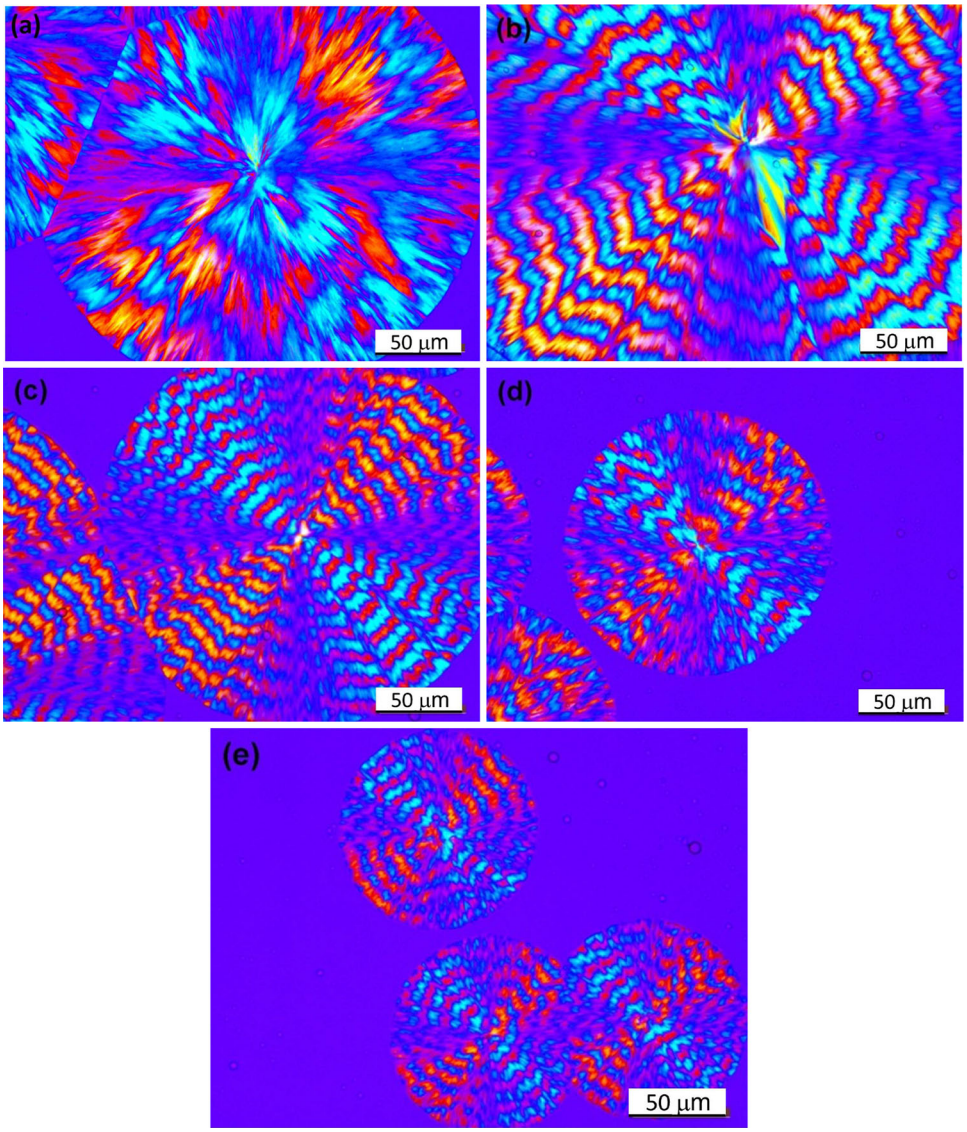

Fig. 11 Spherulitic morphology of PBS and its copolyesters at the identical undercooling ($\Delta T = 34$ °C): **a** PBS, **b** PBS2.5, **c** PBS5, **d** PBS7.5, and **e** PBS10

process. Polymers may form metastable lamellae during crystallization process so that recrystallization is possible during the heating process; the metastable lamellae have the lower melting points as a result of their large surface/volume ratios. Partly to melt, then to recrystallize, a sample could reduce the total free energy of the system by increasing the thickness of the lamellae [30].

The "melting-recrystallization-remelting" process is further confirmed by TMDSC. Compared with conventional DSC, TMDSC, which applies a small sinusoidal oscillation (modulation) on the conventional linear heating programmer, is a very powerful technique to make the total heat flow (THF) to be separated into the heat capacity-related reversible heat flow (RHF) and the kinetic-related heat flow (NHF). This thermal analysis technique has been used in our previous research to investigate the origin of annealing peak of PLLA [31]. The endothermic peak can be observed in both the reversible and nonreversible parts, while the exothermic peak can only be detected in the nonreversible part. So the exotherms (including crystallization and recrystallization) can be separated from glass transitions, reversible melting, or other heat capacity-related events [32, 33]. As shown in Fig. 9b, the exothermic peak, detected in the nonreversible heat flow curve, locates between the low-temperature melting peak and the high-temperature melting peak, implies the existence of melting-recrystallization-melting process.

Equilibrium melting temperature (T_m^o) is the melting temperature of crystals with infinite thickness or segments with infinite length. Many metastable states may form during

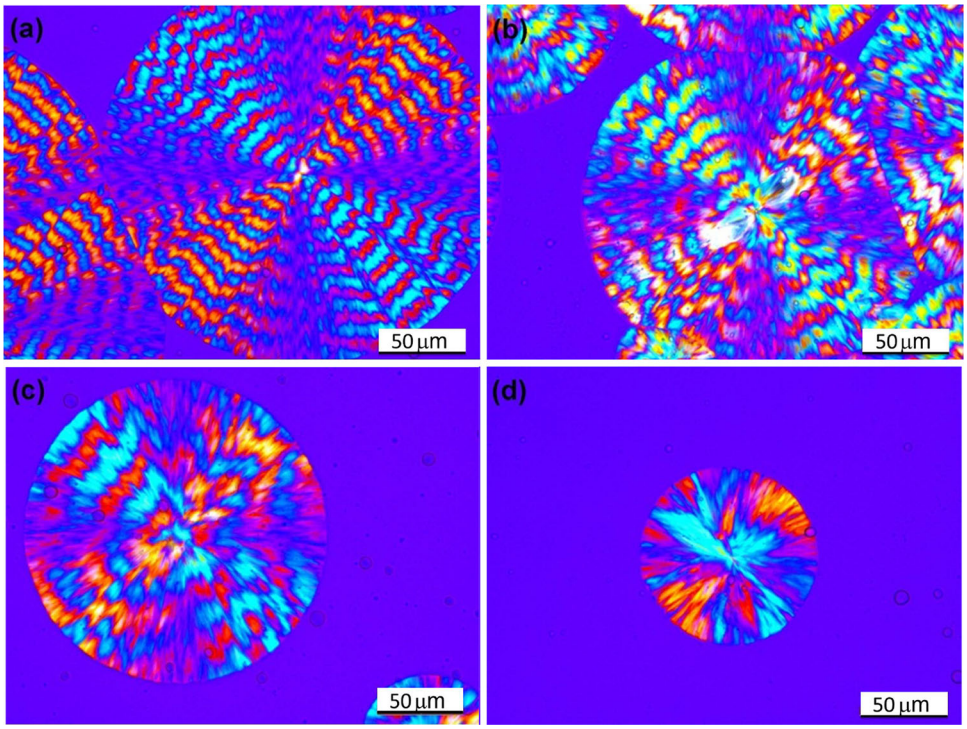

Fig. 12 Spherulitic morphology of PBS5 after isothermal crystallization at various temperatures: **a** 77.5, **b** 80, **c** 82.5 and **d** 85 °C

crystallization process, which make it impossible to obtain the final thermodynamic condition, but T_m^o can be extrapolated from the melting temperature. Here, T_{m1} and T_c will be used to obtain the value of T_m^o. According to the Hoffman-Weeks theory, we can use the following equation [34]:

$$T_m = \frac{T_c}{\gamma} + \left(1 - \frac{1}{\gamma}\right) T_m^o \quad (6)$$

where T_m^o is the equilibrium melting temperature, T_m is donated as the melting temperature of the crystals formed at the given temperature T_c, and γ is a function of the lamellar thickness. Figure 10 shows the observed melting points at different crystallization temperature. For example, the values of T_m^o for PBS and PBS5 are calculated as 119.0 and 112.0 °C, respectively. As expected, hinder effects of DDP unit probably result in the apparently decreasing tendency of T_m^o in PBS copolyesters. With more DDP unit incorporated, the regularity and mobility of chains are restricted deeply, implies that the thickness and the degree of perfection of lamella decrease, so the melting temperatures of crystals decrease subsequently.

Spherulite morphology and growth rate

Figure 11 displays the spherulitic morphologies of PBS copolyesters with different composition at the identical undercooling ($\Delta T = 34$ °C). The typical "Maltese Cross" image and the double-banded extinction patterns appear in all the spherulites. Furthermore, the number of spherulites decreases with the increase in DDP due to the difficulty in nucleation. Compared with neat PBS, PBS10 shows the smallest spherulites, indicating that the special hindrance of DDP reduces the growth rate of crystals.

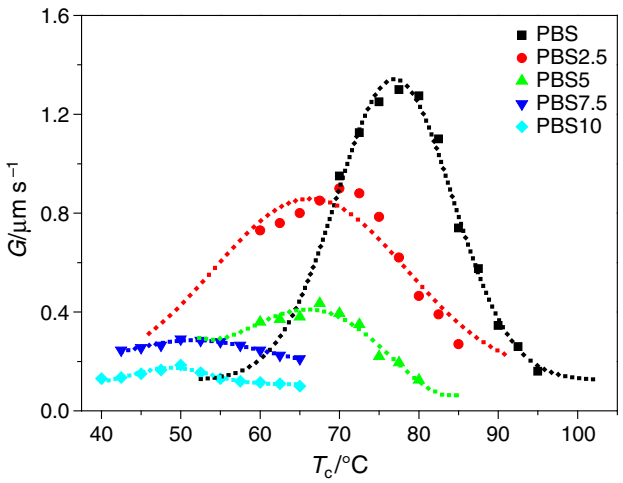

Fig. 13 Spherulitic growth rates of PBS with different composition at different temperatures

The effects of the third component and crystallization temperature on the isothermal melt crystallization of PBS copolyesters are further studied. Figure 12 shows a series

of POM micrographs for PBS5 after isothermal crystallization at different temperatures for 10 min. The sizes of spherulites decrease with the increased temperature, indicating that high crystallization temperature depresses the overall kinetic rates. In addition, we can clearly see that the double-banded extinction patterns appear when the temperature is below 82.5 °C; however, banded spherulites cannot be seen with further increasing the temperature up to 85 °C. It is worth noting that banded spherulite is common in many polymers, which is attributed to the periodic twisting of radiating lamellar crystals [35]. Moreover, the band spacing is found to increase with increasing the temperature, which maybe results from the strain induced by the growing crystals.

In order to further study the growth process of these spherulites, the variation of crystal growth rates of these spherulites with temperatures is evaluated by POM. As we can see in Fig. 13, all curves are in accordance with the Gaussian distribution function. Only at an appropriate given temperature could the crystals grow faster. Besides, comparing the neat PBS, the PBS copolyesters have lower crystal growth rates at the given temperature, indicating that the introduction of DDP depresses the crystal growth rates. For isothermal crystallization, the temperature we chosen was in the regime II or/and regime III, which corresponds to the right side of the bell-shape curves.

Conclusions

Biodegradable poly(butylene succinate) (PBS) copolyesters containing phosphorus groups were synthesized and characterized successfully. Above all, the crystallization and melting behaviors of PBS copolyesters were studied systemically. Due to the hindering effect of DDP, the motion of PBS segment was limited; therefore, crystallization ability of PBS was retarded obviously, especially when the content of DDP exceeds 7.5 mol%. The investigation of isothermal crystallization verified that the crystallization mechanism remains unchanged for PBS copolyesters despite crystallization temperature and the third composition (DDP unit). The higher the crystallization temperature was, the slower the crystallization rates processed, which probably resulted from the lower undercooling of crystallization process. The multiple melting behaviors originated from the "melting-recrystallization-melting," which have been confirmed by TMDSC. The equilibrium temperature decreased with the increasing of DDP content due to the hindering and the dilute effects of the third component. POM analysis revealed that all the copolyesters have lower crystal growth rates than the neat PBS at the given temperature, that is to say, the incorporation of DDP depressed the growth rates of spherulites due to its larger steric hindrance.

Acknowledgements We thank the National Natural Science Foundation of China for financial support (Nos. 31000427, 21034001, 21174021).

References

1. Han HY, Wang XD, Wu DZ. Mechanical properties, morphology and crystallization kinetic studies of bio-based thermoplastic composites of poly(butylene succinate) with recycled carbon fiber. J Chem Technol Biotechnol. 2013;88:1200–11.
2. Miyata T, Masuko T. Crystallization behaviour of poly(tetramethylene succinate). Polymer. 1998;39:1399–404.
3. Wei ZY, Chen GY, Shi YM, Song P, Zhan MQ, Zhang WX. Isothermal crystallization and mechanical properties of poly (butylene succinate)/layered double hydroxide nanocomposites. J Polym Res. 2012;19:9930–40.
4. Soccio M, Lotti N, Munari A. Influence of block length on crystallization kinetics and melting behavior of poly(butylene/thiodiethylene succinate)block copolymers. J Therm Anal Calorim. 2013;114:677–88.
5. Chen L, Wang YZ. A review on flame retardant technology in China. Part I: development of flame retardants. Polym Adv Technol. 2010;21:1–26.
6. Levchik SV, Weil ED. Flame retardancy of thermoplastic polyesters—a review of the recent literature. Polym Int. 2005;54:11–35.
7. Zhang C, Huang JY, Liu SM, Zhao JQ. The synthesis and properties of a reactive flame-retardant unsaturated polyester resin from a phosphorus-containing diacid. Polym Adv Technol. 2011;22:1768–77.
8. Chang SJ, Chang FC. Synthesis and characterization of copolyesters containing the phosphorus linking pendent groups. J Appl Polym Sci. 1999;72:109.
9. Lu SY, Hamerton I. Recent developments in the chemistry of halogen-free flame retardant polymers. Prog Polym Sci. 2002;27:1661–712.
10. Brehme S, Schartel B, Goebbels J, Fischer O, Pospiech D, Bykov Y, Döring M. Phosphorus polyester versus aluminium phosphinate in poly(butylene terephthalate) (PBT): flame retardancy performance and mechanisms. Polym Degrad Stab. 2011;96:875–84.
11. Chang SJ, Sheen YC, Chang RS, Chang FC. The thermal degradation of phosphorus-containing copolymers. Polym Degrad Stab. 1996;54:365–71.
12. Wang DY, Song YP, Lin L, Wang XL, Wang YZ. A novel phosphorus-containing poly(lactic acid) toward its flame retardation. Polymer. 2011;52:233–8.
13. Sablong R, Duchateau R, Koning CE, Pospiech D, Korwitz A, Komber H, Starke S, Häußler L, Jehnichen D, Landwehr MA. Incorporation of a flame retardancy enhancing phosphorus-containing diol into poly(butylene terephthalate) via solid state polycondensation: a comparative study. Polym Degrad Stab. 2011;96:334–41.
14. Li J, Zhu HF, Li J, Fan XY, Tian XY. Thermal degradation behaviors of phosphorus-silicon synergistic flame-retardant copolyester. J Appl Polym Sci. 2011;122:1993–2003.
15. Chang SJ, Chang FC. Sequential distribution of copolyesters containing the phosphorus linking pendant groups characterized by ^{1}H-n.m.r. Polymer. 1998;39:3233–40.
16. Chang SJ, Chang FC. Characterizations for blends of phosphorus-containing copolyester with poly(ethylene terephthalate). Polym Eng Sci. 1998;38:1471–81.
17. Wang DY, Wei LL, Ge XG, Yang KK, Wang XL, Wang YZ. Nonisothermal crystallization behaviors of flame-retardant copolyester/montmorillonite nanocomposites. J Macromol Sci Phys. 2009;48:927–40.

18. Chen HB, Zhang Y, Chen L, Shao ZB, Liu Y, Wang YZ. Novel inherently flame-retardant poly(trimethylene terephthalate) copolymer with the phosphorus-containing linking pendent group. Ind Eng Chem Res. 2010;49:7052–9.
19. Chen HB, Zeng JB, Dong X, Chen L, Wang YZ. Block phosphorus-containing poly(trimethylene terephthalate) copolymer via solid-state polymerization: retarded crystallization and melting behaviour. Cryst Eng Comm. 2013;15:2688–98.
20. Jin TX, Zhou M, Hu SD, Chen F, Fu Q. Effect of molecular weight on the properties of poly(butylene succinate). Chin J Polym Sci. 2014;32:953–60.
21. Tan LC, Chen YW, Zhou WH, Ye SW. crystallization behavior and mechanical strength of poly(butylene succinate-co-ethylene glycol) based nanocomposites using functionalized multiwalled carbon nanotubes. Polym Eng Sci. 2012;52:2506–17.
22. Tan LC, Chen YW, Zhou WH, Nie HR, Li F, He XH. Novel poly(butylene succinate-co-lactic acid) copolymers: synthesis, crystallization, and enzymatic degradation. Polym Degrad Stab. 2010;95:1920–7.
23. Park JW, Kim DK, Im SS. Crystallization behaviour of poly (butylene succinate) copolymers. Polym Int. 2002;51:239–44.
24. Papageorgiou GZ, Bikiaris DN. Crystallization and melting behavior of three biodegradable poly(alkylene succinates). A comparative study. Polymer. 2005;46:12081–92.
25. Yang Y, Qiu ZB. Crystallization kinetics and morphology of biodegradable poly(butylene succinate-co-ethylene succinate) copolyesters: effects of comonomer composition and crystallization temperature. Cryst Eng Comm. 2011;13:2408–17.
26. Wang GY, Qiu ZB. Synthesis, crystallization kinetics and morphology of novel biodegradable poly(butylene succinate-co-hexamethylene succinate) copolyesters. Ind Eng Chem Res. 2012;51:16369–76.
27. Liu XQ, Li CC, Zhang D, Xiao YN. Melting behaviors, crystallization kinetics, and spherulitic morphologies of poly (butylene succinate) and its copolymer modified with rosin maleopimaric acid anhydride. J Polym Sci B Polym Phys. 2006; 44:900–13.
28. Papageorgiou GZ, Achilias DS, Bikiaris DN. Crystallization kinetics of biodegradable poly(butylene succinate) under isothermal and non-isothermal conditions. Macromol Chem Phys. 2007;208:1250–64.
29. Yasuniwa M, Tsubakihara S, Satou T, Iura K. Multiple melting behavior of poly(butylene succinate). II thermal analysis of isothermal crystallization and melting process. J Polym Sci B Polym Phys. 2005;43:2039–47.
30. Xu YX, Xu J, Guo BH, Xie XM. Crystallization kinetics and morphology of biodegradable poly(butylene succinate-co-propylene succinate)s. J Polym Sci B Polym Phys. 2007;45:420–8.
31. Wei ZY, Song P, Zhou C, Chen GY, Chang Y, Li JF, Zhang WX, Liang JC. Insight into the annealing peak and microstructural changes of poly(L-lactic acid) by annealing at elevated temperatures. Polymer. 2013;54:3377–84.
32. Zhang J, Li FX, Yu JY. Multiple melting behavior of biodegradable poly(butylene succinate-co-terephthalate) (PBST) copolymer. J Therm Anal Calorim. 2013;111:711–5.
33. Qiu ZB, Komura M, Ikehara T, Nishi T. DSC and TMDSC study of melting behaviour of poly(butylene succinate) and poly (ethylene succinate). Polymer. 2003;44:7781–5.
34. Gan ZH, Abe H, Kurokawa H, Doi Y. Solid-state microstructures, thermal properties, and crystallization of biodegradable poly (butylene succinate)(pbs) and its copolymers. Biomacromolecules. 2001;2:605–13.
35. Gan ZH, Abe H, Doi Y. Crystallization melting and enzymatic degradation of biodegradable poly(butylene succinate-co-14 mol% ethylene succinate) copolyester. Biomacromolecules. 2001;2:313–21.